Orthogonal Hybrid Waveguides: An Approach to Low Crosstalk and Wideband Photonic Crystal Intersections Design

Kiazand Fasihi and Shahram Mohammadnejad

***Abstract*—A low crosstalk and wideband photonic crystal (PC) waveguide intersection design based on two orthogonal hybrid waveguides in a crossbar configuration is proposed. The finite-difference time-domain (FDTD) and coupled-mode theory (CMT) methods are used to simulate the hybrid waveguides of square lattice. The bandwidth (BW) and crosstalk of the intersection are investigated for various radii of the coupled cavities. It is shown that simultaneous crossing of the lightwave signals through the intersection with negligible interference is possible. The transmission of a 200-fs pulse at 1550 nm is simulated by using the FDTD method, and the transmitted pulse shows negligible crosstalk and very little distortion.**

***Index Terms*—Crosstalk, coupled-mode theory (CMT), finite-difference time-domain (FDTD), orthogonal hybrid waveguides, photonic crystal (PC) intersections.**

I. Introduction

RECENTLY, photonic crystals (PCs) have attracted great interests due to their potential ability of controlling light propagation with the existence of photonic bandgap (PBG), and the possibilities of implementing compact optical integrated circuits [1]–[6]. Waveguide intersections with low crosstalk and high BW are the key element for implementation of integrated photonic circuits. In 1998, Johnson *et al.* proposed a scheme to eliminate crosstalk for a waveguide intersection based on a two-dimensional (2-D) PC of square lattice by using a single defect with doubly degenerate modes [7]. They also presented general criteria for designing such waveguide intersections based on symmetry consideration. Lan and Ishikawa presented another mechanism where the defect coupling is highly dependent on the field patterns in the defects and the alignment of the defects (i.e., the coupling angle) [8]. They asserted that their design leads to a 10-nm wide region at the central wavelength of 1310 nm with crosstalk as low as -10 to -45 dB, while in [7] the width of the transmission band with comparable crosstalk is only 7.8 nm. In the aforementioned design, the central wavelength value of the low crosstalk transmission band is related to the air-holes radii of PC structure and therefore, adjusting the wavelength domain of transmission band is a challenge. Furthermore, Liu *et al.* proposed another waveguide intersection for lightwaves with no crosstalk and excellent transmission which was based on nonidentical PC coupled resonator optical waveguide (CROW), without transmission band overlap [9].

Zhaofeng *et al.* proposed a different approach that utilizes a vanishing overlap of the propagation modes in the waveguides created by line defects which support dipole-like defect modes [10]. They claimed that in their design, over a BW of 30 nm with the central wavelength at 1300 nm, transmission efficiency above 90% with crosstalk below -30 dB can be obtained. It is obvious that in that proposal—and also in [9], simultaneous propagation of lightwaves with equal frequencies through the intersection is impossible and due to using of taper structure to solve the mode mismatch problem, total length of the intersection is increased. In our solution, an approach to design of low crosstalk and wideband PC waveguide intersections based on two orthogonal hybrid waveguides in a crossbar configuration, is proposed. The paper is organized as follows: In Section II, the hybrid waveguides are introduced and analyzed using coupled-mode theory (CMT) method. Fundamental approach to low crosstalk and wideband intersections design is proposed in Section III. In Section VI, the orthogonal hybrid waveguide intersections are simulated using the FDTD method. Also, simultaneous crossing of lightwave signals and transmission of ultrashort pulses through the proposed intersection are investigated.

II. Theoretical Model for Hybrid Waveguides: CMT Approximation

A. Hybrid Waveguides

The PC-based coupled cavity waveguides (CCW) are formed by placing a series of high-Q optical cavities close together. In this case, due to weak coupling of the cavities, light will be transferred from one cavity to its neighbors and a waveguide can be created [11]. By combining the CCWs and the conventional line defect waveguides a new waveguide can be created, which is referred to as hybrid waveguide. Fig. 1 shows the structures of a hybrid waveguide and an orthogonal hybrid waveguide intersection which are implemented in a square lattice PC. Usually, for various applications such as ultrashort pulse transmission, there is a need to have a large BW and a quasi-flat transmission spectrum within the transmission band. If the confinement of the coupled cavities is increased, the continuous transmission band will be converted to a series of discrete bands,

Manuscript received March 15, 2008; revised July 21, 2008. Current version published April 17, 2009.

The authors are with the Department of Electrical Engineering, Iran University of Science and Technology, Nanoptronics Research Center, Tehran, Iran (e-mail: kfasihi@iust.ac.ir; shahramm@iust.ac.ir).

Color versions of one or more of the figures in this paper are available online at http://ieeexplore.ieee.org.

Digital Object Identifier 10.1109/JLT.2008.929422

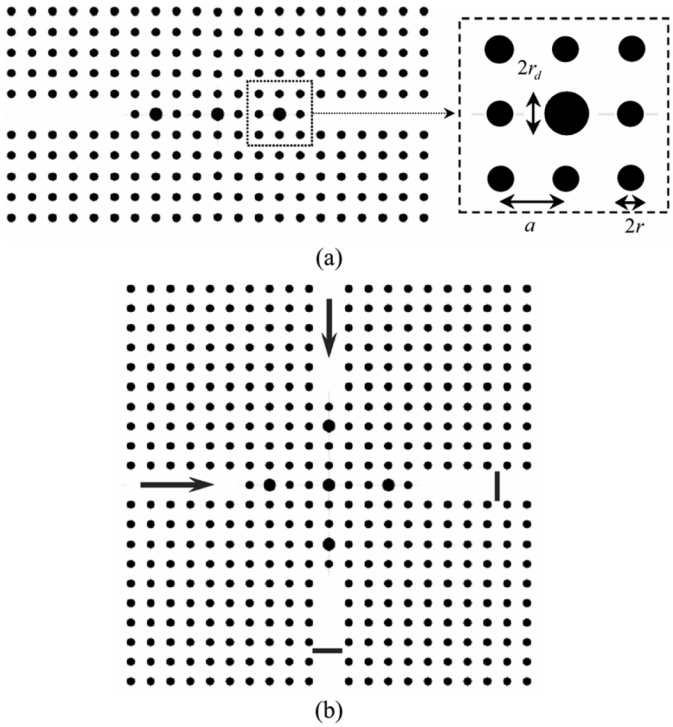

Fig. 1. Schematic structures of square lattice PC components studied in this paper. (a) A hybrid waveguide (a, r and r_d are the lattice constant, the radius of the dielectric rods, and the radius of the coupled cavities, respectively) and (b) an orthogonal hybrid waveguide intersection.

which are useful for implementation of some optical devices, such as filters [12]. Generally, there are two types of PC lattice structures, air-hole-type and rod-type. Despite easier fabrication of PC waveguide based on air-hole-type structures than rod-type waveguides, there are limitations on frequency BW of the single mode region and the group velocity [13]. Moreover in PC waveguides based on rod-type structure the wide BW and large group velocity can be achieved, and recently such waveguides have been used for fabrication of photonic devices [14].

B. Modeling of Hybrid Waveguides by CMT Method

Here, we consider the CCWs that are formed by periodically introducing defects along one direction. The corresponding model which contains N identical defects is schematically shown in Fig. 2. According to CMT, the equations describing the energy amplitude of ith PC defect, a_i $(i = 1, \ldots, N)$, can be written as [15]

$$\frac{\mathrm{d}}{\mathrm{dt}}(a_i) = \left(j\omega_0 - \frac{2}{\tau}\right) a_i + \sqrt{\frac{2}{\tau}} s_{+i} + \sqrt{\frac{2}{\tau}} s'_{+i} \tag{1a}$$

$$s_{-i} = -s_{+i} + \sqrt{\frac{2}{\tau}} a_i$$

$$s'_{-i} = -s'_{+i} + \sqrt{\frac{2}{\tau}} a_i \tag{1b}$$

where ω_0 is the resonant frequency of the PC defects and $1/\tau$ denotes the external decay rate of a_i into one of its two adjacent defects. Here, the internal loss of energy in PC defects is ignored. As shown in Fig. 2, s_{+i} and s'_{+i} are the electromagnetic waves entering into the ith PC defect from its left and right sides, respectively. Also, s_{-i} and s'_{-i} represent the electromagnetic waves emerging from the left and right sides of the i th PC defect, respectively. The coupling between two PC cavities depends on the leakage rate of energy amplitude into the adjacent cavity $(1/\tau)$, which defines the quality factor of the cavity, and the phase-shift of the electromagnetic wave traveling between two adjacent cavities (φ). It can be shown that in a straight CCW which contains N PC cavities $(N > 3)$, the transmission spectrum is given as [15]

$$T_N = \Big(\left[(\alpha^2 - \sin^2\varphi) A_{N-2} - 2\alpha A_{N-3} + A_{N-4} \right]^2 \times (2\sin\varphi)^{-2} + \left[-\alpha A_{N-2} + A_{N-3} \right]^2 \Big)^{-1} \tag{2}$$

where

$$\alpha = 4Q\,(\omega/\omega_0 - 1)\sin\varphi - \cos\varphi$$
$$Q = (\omega_0 \tau)/4. \tag{3}$$

In the above equation, ω, ω_0 and Q are the frequency of incident input, the resonant frequency and the quality factor of PC cavities, respectively. In (2), A is a series function of $\beta = (\alpha - \cos\varphi)$ that satisfies $A_{-1} = 0, A_0 = 1$ and $A_m = \beta A_{m-1} - A_{m-2} (m = 1, 2, 3, \ldots, N)$. As shown in (2), apart from ω, the transmission spectrum of a CCW depends on three parameters ω_0, Q and φ. The ω_0 and Q, can be extracted from a simple numerical simulation on a PC molecule, composed of two coupled cavities. For $N = 2$, i.e., a PC molecule, the transmission spectrum is given as

$$T_2 = \left(T_{\min}^{-1} - 8Q^2 \cos^2\varphi \left(\frac{\omega}{\omega_0} - \frac{1}{4Q\tan\varphi} - 1 \right)^2 + 64Q^4 \sin^2\varphi \left(\frac{\omega}{\omega_0} - \frac{1}{4Q\tan\varphi} - 1 \right)^4 \right)^{-1} \tag{4}$$

where

$$T_{\min} = 4\left(2 + \sin^{-2}\varphi + \sin^2\varphi\right)^{-1}. \tag{5}$$

In the above equations, $T_{\min}$ is the minimum in transmission band of a PC molecule. The peaks of the (4), which are equal to unity, appear at $\omega = \omega_0$ and $\omega = \omega_0 \left[1 + (2Q\tan\varphi)^{-1}\right]$. Hence, using (5) and the simulated transmission spectrum of one PC molecule, ω_0 and Q can be extracted. It must be noted that the analytical results of (2) can be extended to CCWs of any dimensions [15]. Now, we consider the hybrid waveguides that contain N identical cavities in 2-D-PCs and generalize CMT analytical method to obtain the transmission spectrum. According to (2), it can be seen that for a given N, the transmission spectrum curve has $2N - 1$ number of extremums and the minimum in transmission spectrum $T_{\min}$ is independent of ω_0 and

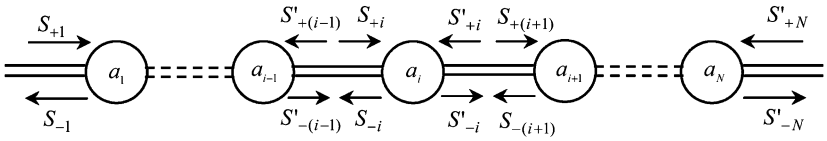

Fig. 2. Schematic diagram for CCWs based on CMT [15].

TABLE I
VALUES OF THE MINIMUM IN THE HW3 TRANSMISSION SPECTRUM FOR VARIOUS RADII OF THE COUPLED CAVITIES

r_d	$T_{\min}$	r_d	$T_{\min}$
0.270*a*	**0.8831**	**0.3075*a***	**0.8463**
0.275*a*	**0.7311**	**0.310*a***	**0.5700**
0.280*a*	**0.4911**	**0.315*a***	**0.3112**
0.285*a*	**0.3619**	**0.320*a***	**0.1870**
0.290*a*	**0.3297**	**0.325*a***	**0.1669**
0.295*a*	**0.4552**	**0.330*a***	**0.2334**
0.300*a*	**0.6170**	**0.335*a***	**0.3997**
0.3025*a*	**0.8894**	**0.340*a***	**0.2773**
0.305*a*	**0.8958**	**0.345*a***	**0.3681**

Q. Therefore, we can obtain φ as a function of the radius of the coupled cavities r_d as follows.

- The relationship between $T_{\min}$ and r_d can be calculated by repeating a numerical simulation, such as FDTD method, for different values of r_d.
  Here we consider a hybrid waveguide which contains three coupled cavities, $N = 3$ [see Fig. 1(a)], in the 2-D-PC of square lattice composed of dielectric rods in air. Now, we have chosen to name this hybrid waveguide HW3 and extend this naming to other hybrid waveguides. The rods have refractive index $n_{\text{rod}} = 3.4$ and radius $r = 0.20a$, where a is the lattice constant. By normalizing every parameter with respect to the lattice constant a, we can scale the waveguide structure to any length scale simply by scaling a. The radius of the coupled cavities are varied from $0.27a$ to $0.345a$. The grid size parameter in the FDTD simulation is set to $0.046a$ and the excitations are electromagnetic pulses with Gaussian envelope, which are applied to the input port from the left side. All the FDTD simulations below are for TM (i.e., with electric field parallel to the rod axis) polarization. The field amplitude is monitored at suitable location at the right side of the HW3. Table I shows the relationship between $T_{\min}$ and r_d for the HW3 which are obtained from the FDTD simulations.
- The relationship between $T_{\min}$ and φ for the HW3 can be calculated from (2).

Fig. 3 shows this relationship over one-half period of (2).

Therefore, the relationship between φ and r_d of the HW3 can be demonstrated in Fig. 4. In order to compare the results of CMT and FDTD methods, we consider a HW2 under the same conditions as mentioned previously and utilize the FDTD simulation results to compute ω_0 and Q. The radius of the coupled cavities are set to $r_d = 0.32a$. The transmission spectrum of HW2 computed by the FDTD is shown in Fig. 5. According to this figure, the parameters ω_0, Q and φ are equal

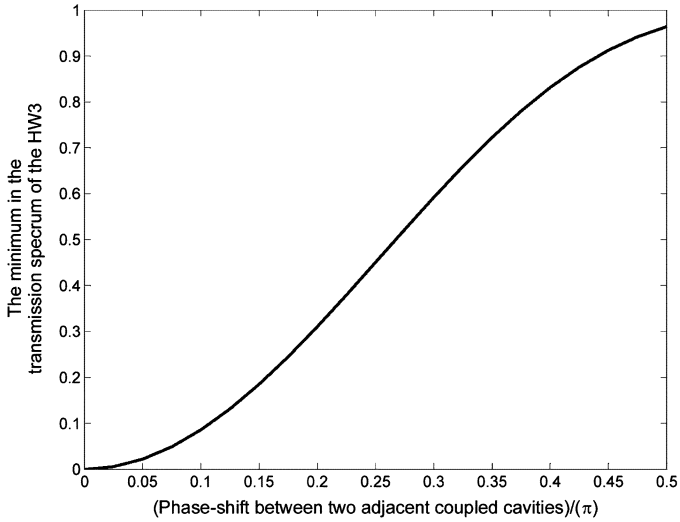

Fig. 3. The relationship between $T_{\min}$ and φ in the HW3.

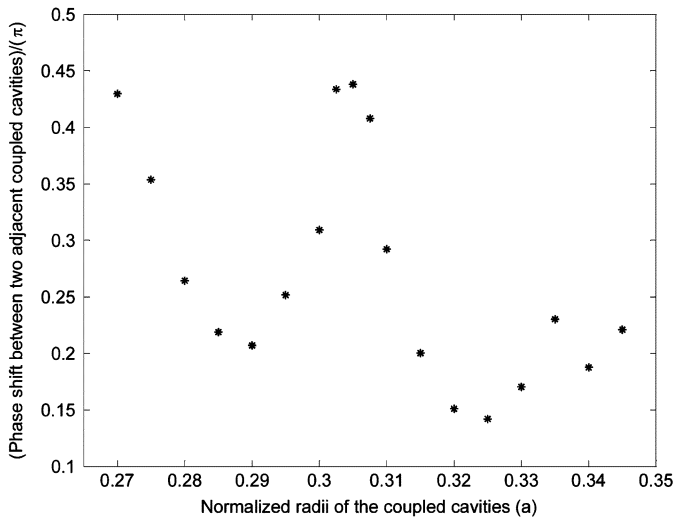

Fig. 4. The phase-shift between two adjacent cavities as a function of radius of the coupled cavities in the HW3.

to $0.3428\ (a/\lambda)$, 130.3, and 0.4066π, respectively. Hence, the CMT transmission spectrum can be calculated from (4) (see Fig. 5). It is observed that the transmission spectrum calculated by CMT is in good agreement with that simulated by FDTD. As another example, we take a HW3 under the same condition as mentioned previously, with $r_d = 0.32a$ which corresponds to $\varphi = 0.1509\,\pi$. The transmission spectra of the above HW3 simulated by FDTD and CMT are shown in Fig. 6 for comparison. Although there is a difference in the minimum transmission spectrum between the first and second peaks, it is observed that

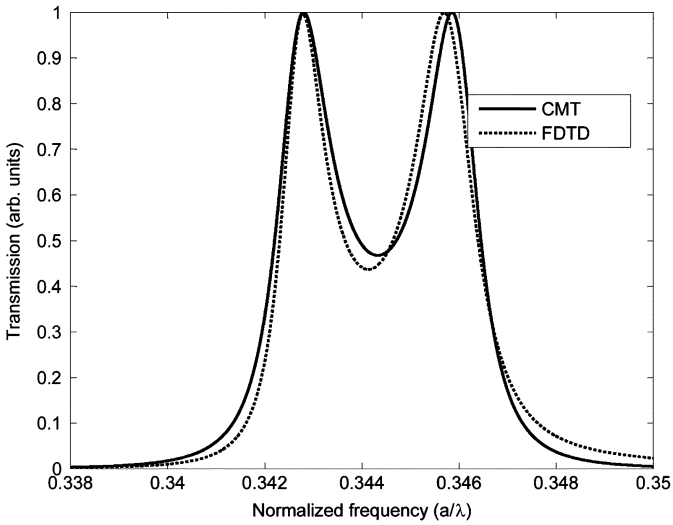

Fig. 5. The simulation results of transmission spectrum of the HW2 obtained by the FDTD method (the dotted curve) and the CMT method (the solid curve).

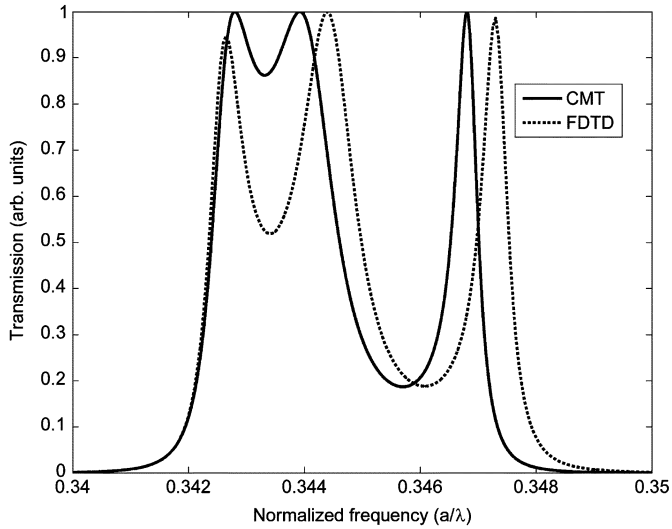

Fig. 6. The simulation results of transmission spectrum of the HW3 obtained by (a) the FDTD method (the dotted curve) and (b) the CMT method (the solid curve).

the spectrum calculated by analytical method is nearly in good agreement with that simulated by the numerical simulation.

III. Fundamental Approach To Low Crosstalk and Wideband Intersections Design in Square Lattice PCs

In this section, we first consider the basic criteria proposed in [7] to eliminate crosstalk in waveguide intersections, and then generalize it for two orthogonal hybrid waveguides in a crossbar configuration. Johnson *et al.* presented general criteria based on symmetry for the intersection with high throughput and very low crosstalk. The criteria are as shown here.

- Each waveguide must have a mirror symmetry plane through its axis and perpendicular to the other waveguide and have a single guided mode in the frequency range of interest. This mode will be either even or odd with respect to the mirror plane.
- The center of the intersection must be occupied by a resonant cavity that is symmetric with respect to the mirror planes of both waveguides.
- Two resonant modes must exist in the cavity, each of which is even with respect to one waveguide's mirror plane and odd with respect to the other. These modes should be the only resonant modes in the frequency range of interest.

The fundamental idea is to consider coupling of the four branches of the intersection in terms of a single resonant cavity at the center. If the above conditions are satisfied, then each resonant state of the cavity will couple to modes in just one waveguide and be orthogonal to modes in the other waveguide. So, assuming that the branches only couple to one another through the resonant cavity, crosstalk will be eliminated. But the FDTD calculated transmission spectra of the intersections, which are based on a single cavity at the center of the intersection of two line-defect waveguides, show that under the best circumstances for several structural variations, only a narrow low crosstalk wavelength region can be obtained [7].

We can generalize these criteria to the structure of Fig. 1(b), which is based on two orthogonal HW3s in a crossbar configuration. In this structure, by photon hopping through the coupled cavities, light can propagate from one branch to the other branches. Since the structure of the proposed intersection satisfies the criteria of the [7], we can find wavelength region with very low crosstalk. In this structure the BW is determined by interaction of the individual resonant frequencies of the coupled cavities. It will be shown that in the case of $\varphi \approx (k + 1/2)\,\pi$, where k is an integer including zero, a quasi-flat impurity band can be achieved. Consequently, a wideband and low crosstalk intersection with high transmission efficiency can be obtained.

IV. Simulation and Results

A. Simulation of the Orthogonal Hybrid Waveguide Intersections by FDTD Method

Without losing generality, once again we consider a 2-D square lattice of infinitely long dielectric rods in air. The rods have refractive index $n_{\mathrm{rod}} = 3.4$ and radius $r = 0.20a$. These parameters lead to a PBG for the TM mode from $a/\lambda_0 = 0.2876$ to 0.4228, here λ_0 is the free-space wavelength. To determine the PBG regions of the PC structure, the MIT Photonic-Bands package [16] is used. To evaluate the performance of the proposed device, the FDTD method is used for simulation, under the same conditions as mentioned previously. The excitations are electromagnetic pulses with Gaussian envelope, which are launched to the input port from the left side. The field amplitudes are monitored at suitable locations around the intersection in horizontal and perpendicular waveguides. Fig. 7(a) and (b) shows the transmission and crosstalk characteristics of the orthogonal HW3 intersection, where the radius of the coupled cavities are set to $r_d = 0.28a$ and $r_d = 0.32a$,, respectively. As can be seen from Fig. 7(a) and (b), there exists around $0.0415a$ and $0.0228a$ regions in which the transmission is over 50%. Also, it must be noted that the transmission properties of the proposed intersection are the same as transmission properties of the corresponding hybrid

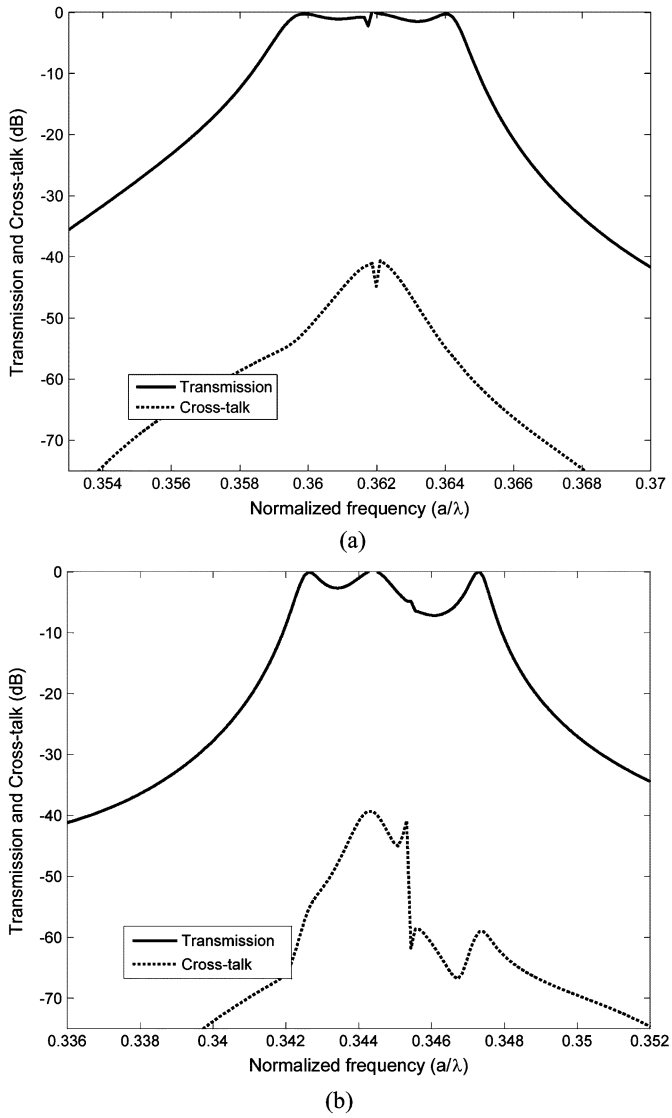

Fig. 7. The transmission and crosstalk characteristics of the orthogonal HW3 intersection when the radius of the coupled cavities are set to (a) $r_d = 0.28a$ and (b) $r_d = 0.32a$.

TABLE II
VALUES OF THE TRANSMISSION REGION, −3 DB BW AND CROSSTALK IN ORTHOGONAL HW3 INTERSECTION FOR VARIOUS RADII OF THE COUPLED CAVITIES

Radius of cavities	Transmission region (a/λ)	$-3dB$ BW (in terms of wavelength)	$-3dB$ BW for $a = 0.55\mu m$	Cross-talk range (dB)	
0.27*a*	**0.3861-0.3932**	**0.0468*a***	**25.7 nm**	**-34.35**	**-41.74**
0.28*a*	**0.3769-0.3829**	**0.0415*a***	**22.8 nm**	**-32.16**	**-47.60**
0.29*a*	**0.3680-0.3734**	**0.0393*a***	**21.6 nm**	**-33.39**	**-52.76**
0.30*a*	**0.3592-0.3645**	**0.0404*a***	**22.2 nm**	**-40.19**	**-53.42**
0.3025*a*	**0.3569-0.3624**	**0.0425*a***	**23.4 nm**	**-43.96**	**-55.06**
0.305*a*	**0.3545-0.3601**	**0.0438*a***	**24.1 nm**	**-45.35**	**-55.05**
0.3075*a*	**0.3522-0.3579**	**0.0452*a***	**24.9 nm**	**-46.66**	**-56.23**
0.31*a*	**0.3503-0.3555**	**0.0417*a***	**22.9 nm**	**-46.16**	**-55.58**
0.32*a*	**0.3423-0.3450**	**0.0228*a***	**12.5 nm**	**-39.34**	**-59.21**
0.33*a*	**0.3348-0.3381**	**0.0291*a***	**16.0 nm**	**-35.61**	**-60.89**
0.34*a*	**0.3272-0.3305**	**0.0305*a***	**16.8 nm**	**-38.79**	**-50.27**

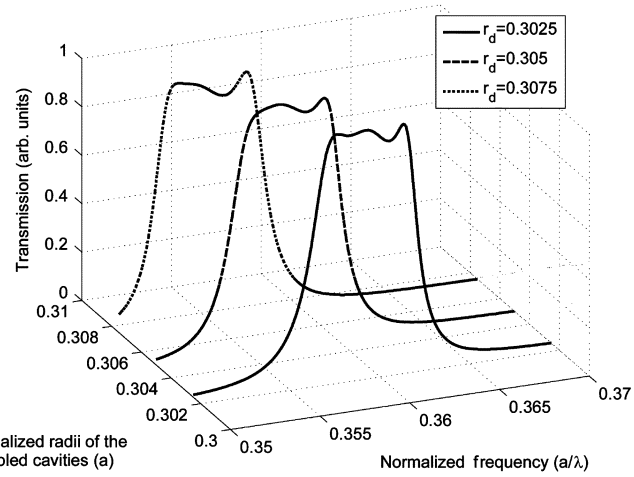

Fig. 8. The transmission behavior of the orthogonal HW3 intersection when $\varphi \approx (k + 1/2)\pi$.

waveguide. Furthermore, by varying the radius of the coupled cavities of the hybrid waveguides, a wide frequency domain of transmission band will be obtained which proves the flexibility of the proposed design. Table II, shows the transmission region, -3dB BW and the crosstalk of the proposed intersection for different values of the coupled cavities radii. Assuming the lattice constant $a = 0.55$ μm, considering that in this case the center wavelength of transmission band is equal to 1550 nm when $r_d = 0.3075a$, the intersection BWs for different radius of the coupled cavities at working wavelength of 1550 nm can be obtained and is shown in the column 4 of Table II. By comparing the results of Fig. 4 and Table II, it can be seen that the optimum values of BW and crosstalk are obtained when $\varphi \approx (k + 1/2)\pi$. In this case, the transmission spectra of the intersection is quasi-flat (see Fig. 8).

B. Simultaneous Crossing of Lightwave Signals and Transmission of Ultrashort Pulses Through the Orthogonal Hybrid Waveguide Intersections

In the implementation of PC-based integrated circuits, such as those which used in wavelength division multiplexing (WDM) systems, it is necessary to have intersections in which simultaneous crossing of lightwaves is possible. In the orthogonal hybrid waveguide intersections, lightwave signals can cross through the intersection simultaneously because each resonant state of the intersection will couple to modes in just one waveguide and be orthogonal to modes in the other waveguide. We consider the structure shown in Fig. 1(b) and verify this idea by using the FDTD technique. In this simulation, the radius of the coupled cavities of the orthogonal HW3 are chosen to be $r_d = 0.3075a$ where $a = 0.55$ μm. During simulation, two input pulses with Gaussian envelope are applied to input ports from the top and the left sides. The monitors are placed at right and bottom output ports at suitable locations. The intensities of 500-fs pulses are adjusted to unity and 0.5, while their central wavelengths are set at 1550 nm and the phase

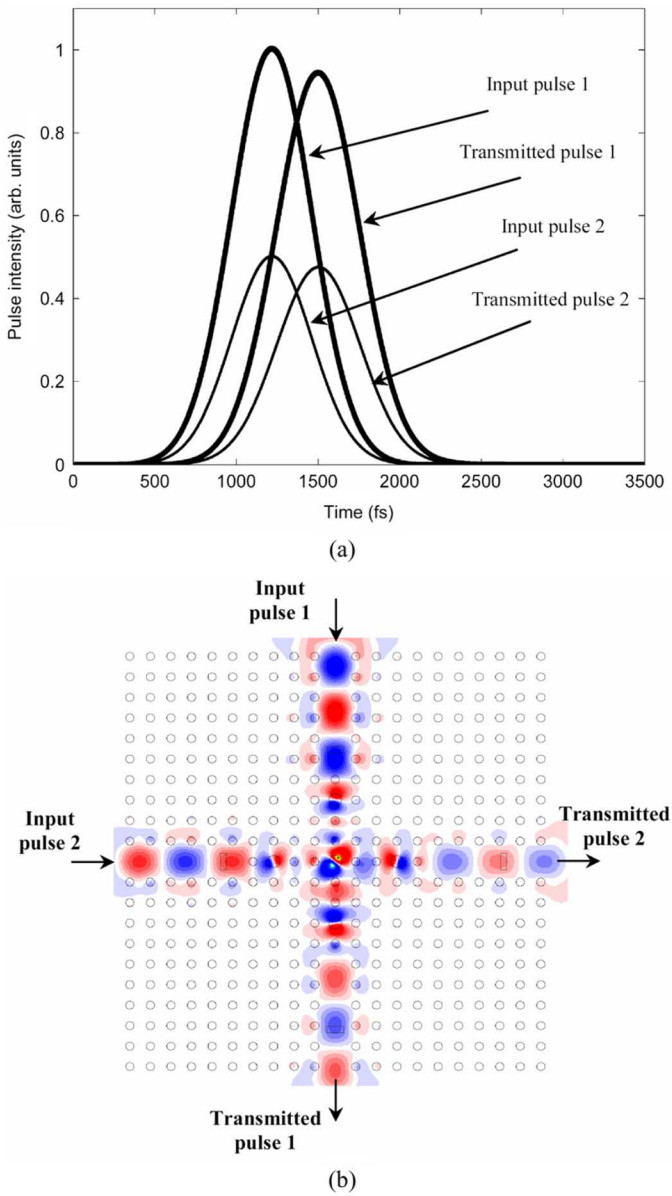

Fig. 9. The simultaneous crossing of two lightwave signals through the orthogonal HW3 intersection with $r_d = 0.3075a$ and $a = 0.55$ μm. (a) Calculated transmission spectra. (b) Calculated field distribution. The intensities of 500-fs pulses are adjusted to unity and 0.5, while their central wavelengths are set at 1550 nm and the phase difference between them is 180°.

difference between them is 180 °. Fig. 9 shows the transmission behavior of simultaneous crossing of lightwave signals through the orthogonal HW3 intersection. It can be seen that the input pulses are transmitted through the intersection with negligible interference effect. In a separate assessment, we again consider the structure shown in Fig. 1(b) with $r_d = 0.3075a$ where $a = 0.55$ μm, and investigate the transmission property of the intersection for ultrashort pulses by using the FDTD method.

Fig. 10 shows the transmission behavior of a 200-fs pulse whose central wavelength is 1550 nm. We can see that not only the crosstalk is negligible, but also the distortion of the pulse shape is very small.

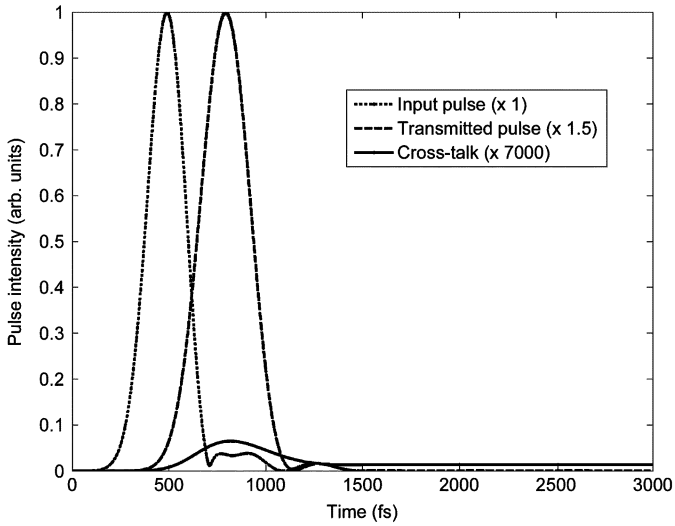

Fig. 10. The transmission behavior of a 200-fs pulse whose central wavelength is 1550 nm through the orthogonal HW3 intersection with $r_d = 0.3075a$ and $a = 0.55$ μm.

V. Conclusion

In this paper, a low crosstalk and wideband waveguide intersection design based on two orthogonal hybrid waveguides in crossbar configuration was proposed and modeled by using the FDTD and CMT methods. It has been demonstrated that the theoretical results derived by CMT for simulation of the hybrid waveguides are in good agreement with FDTD simulation results. Also, it has been shown that when the phase-shift of the electromagnetic waves traveling between two adjacent PC coupled cavities is approximately equal to $(k+1/2)\pi$, i.e., quasi-flat condition, optimum performance results for the intersection can be achieved. In addition, it has been clearly proved that simultaneous crossing of ultrashort pulses through the intersection is possible with negligible interference. The proposed solution can be easily generalized to other 2-D square as well as 3-D cubic PCs.

References

[1] J. D. Joannopoulos, R. D. Meade, and J. N. Winn, *Photonic Crystals: Molding the Flow of Light*. Princeton, NJ: Princeton Univ. Press, 1995.

[2] M. F. Yanik, H. Altug, J. Vuckovic, and S. Fan, "Submicometer all-optical digital memory and integration of nanoscale photonic devices without isolator," *J. Lightw. Technol.*, vol. 22, pp. 2316–2322, Oct. 2004.

[3] T. Niemi, L. H. Frandsen, K. K. Hede, A. Harpøth, P. I. Borel, and M. Kristensen, "Wavelength-division demultiplexing using photonic crystal waveguides," *IEEE Photon. Technol. Lett.*, vol. 18, pp. 226–228, Jan. 2006.

[4] M. Koshiba, "Wavelength division multiplexing and demultiplexing with photonic crystal waveguide coupler," *J. Lightw. Technol.*, vol. 19, pp. 1970–1975, Dec. 2001.

[5] T. Niemi, L. H. Frandsen, K. K. Hede, A. Harpøth, P. I. Borel, and M. Kristensen, "Wavelength-division demultiplexing using photonic crystal waveguides," *IEEE Photon. Technol. Lett.*, vol. 18, pp. 226–228, Jan. 2006.

[6] M. Davanço, A. Xing, J. W. Rarig, E. L. Hu, and D. J. Blumenthal, "Compact broadband photonic crystal filters with reduced back-reflections for monolithic INP-based photonic integrate circuits," *IEEE Photon. Technol. Lett.*, vol. 18, pp. 1155–1157, May 2006.

[7] S. J. Johnson, C. Manolatou, S. Fan, P. R. Villeneuve, J. D. Joannopoulos, and H. A. Haus, "Elimination of crosstalk in waveguide intersections," *Opt. Lett.*, vol. 23, pp. 1855–1857, Dec. 1998.

[8] S. Lan and H. Ishikawa, "Broadband waveguide intersections with low cross talk in photonic crystal circuits," *Opt. Lett.*, vol. 27, pp. 1567–1569, Sep. 2002.
[9] T. Liu, M. Fallahi, M. Mansuripour, A. R. Zakharian, and V. Moloney, "Intersection of nonidentical optical waveguides based on photonic crystals," *Opt. Lett.*, vol. 30, pp. 2409–2411, Sep. 2005.
[10] Z. Li, H. Chen, J. Chen, F. Yang, H. Zheng, and S. Feng, "A proposal for low crosstalk square-lattice photonic crystal waveguide intersection utilizing the symmetry of waveguide modes," *Opt. Commun.*, vol. 273, pp. 89–93, Dec. 2007.
[11] A. Yariv, Y. Xu, R. Lee, and A. Scherer, "Coupled-resonator optical waveguide: A proposal and analysis," *Opt. Lett.*, vol. 24, pp. 711–713, Jun. 1999.
[12] W. Ding, L. Chen, and S. Liu, "Localization properties and the effects on multi-mode switching in discrete mode CCWs," *Opt. Commun.*, vol. 248, pp. 479–484, Dec. 2004.
[13] T. Fujisawa and M. Koshiba, "Finite-element modeling of nonlinear Mach-Zehnder interferometers based on photonic- crystal waveguides for all-optical signal processing," *J. Lightw. Technol.*, vol. 24, pp. 617–623, Jan. 2006.
[14] C. C. Chen, C. Y. Chen, W. K. Wang, F. H. Huang, C. K. Lin, W. Y. Chiu, and Y. J. Chan, "Photonic crystal directional couplers formed by InAlGaAs nano-rods," *Opt. Expr.*, vol. 13, pp. 38–43, Jan. 2005.
[15] L. X. Sheng, C. X. Wen, and L. Sheng, "Analysis and engineering of coupled cavity waveguides based on coupled-mode theory," *Chin. Phys. Soc./IOP* , vol. 14, pp. 2033–2040, Oct. 2005.
[16] [Online]. Available: http://ab-initio.mit.edu/mpb

Kiazand Fasihi was born in 1977. He received the B.Sc. degree from Razi University and the M.Sc. degree from Iran University of Science and Technology (IUST).

He is currently working toward the Ph.D. degree at IUST where his research interests include photonic crystal devices and optical integrated circuits.

Shahram Mohammadnejad received the B.Sc. degree in electrical engineering from the University of Houston, Houston, TX, in 1981 and the M.Sc. and Ph.D. degrees in semiconductor material growth and lasers from Shizuoka University, Shizuoka, Japan, in 1990 and 1993, respectively.

He invented the PdSrS laser for the first time in 1992. He has published more than 80 scientific papers and books. His research interests include semiconductor material growth, quantum electronics, semiconductor devices, optoelectronics, and lasers.

Dr. Mohammadnejad is a scientific committee member of the Iranian Conference of Electrical Engineering (ICEE), a member of Institute of Engineering and Technology (IET), and a member of IET- CEng.